Volume 22
Number 18
21 September 2022
Pages 3281–3570

Lab on a Chip

Devices and applications at the micro- and nanoscale

rsc.li/loc

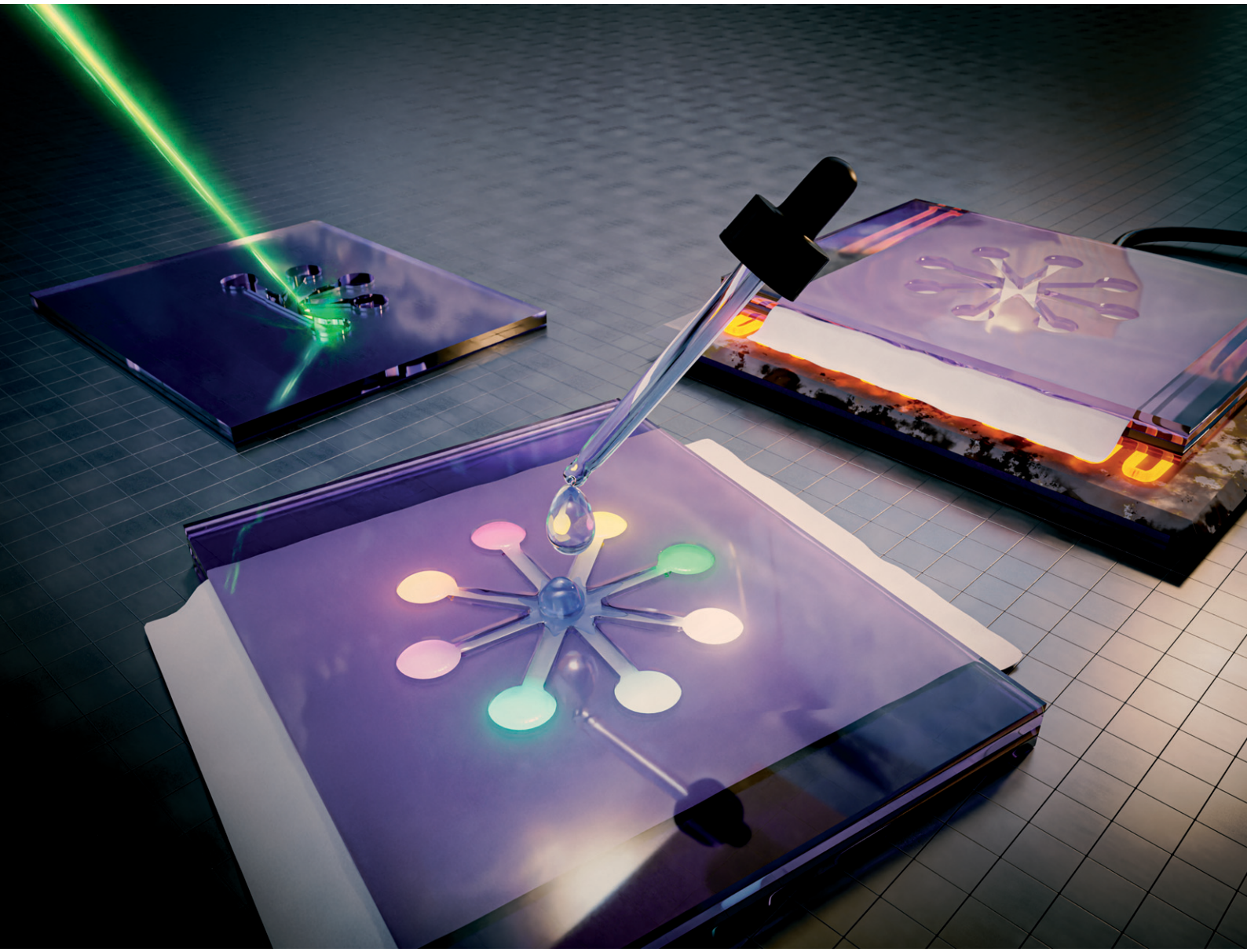

ISSN 1473-0197

ROYAL SOCIETY OF CHEMISTRY

PAPER

Nityanand Kumawat *et al.*
Rapid and inexpensive process to fabricate paper based microfluidic devices using a cut and heat plastic lamination process

Lab on a Chip

PAPER

View Article Online
View Journal | View Issue

Cite this: *Lab Chip*, 2022, **22**, 3377

Rapid and inexpensive process to fabricate paper based microfluidic devices using a cut and heat plastic lamination process

Nityanand Kumawat, *[a] Soja Saghar Soman, [a] Sanjairaj Vijayavenkataraman [ab] and Sunil Kumar [ab]

Microfluidic paper-based analytical devices (microPADs) are emerging as simple-to-use, low-cost point-of-care testing platforms. Such devices are mostly fabricated at present by creating hydrophobic barriers using wax or photoresist patterning on porous paper sheets. Even though devices fabricated using these methods are used and tested with a wide variety of analytes, still they pose many serious practical limitations for low-cost automated mass fabrication for their widespread applicability. We present an affordable and simple two-step process – cut and heat (CH-microPADs) – for the selective fabrication of hydrophilic channels and reservoirs on a wide variety of porous media such as tissue/printing/filter paper and cloth types, such as cotton and polyester, by a lamination process. The technique presents many advantages as compared to existing commonly used methods. The devices possess excellent mechanical strength against bending, folding and twisting, making them virtually unbreakable. They are structurally flexible and show good chemical resistance to various solvents, acids and bases, presenting widespread applicability in areas such as clinical diagnostics, biological sensing applications, food processing, and the chemical industry. Fabricated paper media 96 well-plate CH-microPAD configurations were tested for cell culture applications using mice embryonic fibroblasts and detection of proteins and enzymes using ELISA. With a simple two-step process and minimal human intervention, the technique presents a promising step towards mass fabrication of inexpensive disposable diagnostic devices for both resource-limited and developed regions.

Received 17th May 2022,
Accepted 20th June 2022

DOI: 10.1039/d2lc00452f

rsc.li/loc

Introduction

Microfluidic paper-based analytical devices (microPADs) were first reported in 2007 using lithographical protocols for patterning on a paper sheet.[1] MicroPADs are fabricated by creating hydrophobic barriers on the paper sheet to create hydrophilic channels and test areas to guide the analytes of interest in a specific direction to the point of interest. As compared to conventional microfluidic devices, microPADs present many distinct advantages such as low-cost, smaller size, and ability to function without supporting equipment such as pumps and power sources due to the intrinsic capillary action of porous paper.[2] The miniaturization of multiple laboratory functions into paper-based chips integrated with faster responses has opened up new opportunities in the field of low-cost portable point of care diagnostics.[3–5] MicroPADs have shown potential use for various fluidic applications such as food safety and processing,[6–11] environmental monitoring,[11–15] cell biology,[14,16] drug screening[17,18] and clinical diagnosis.[11,19–22]

Several techniques have been demonstrated in the literature to pattern paper substrates for the fabrication of microPADs. Fundamentally, the shapes of microfluidic pathways, such as channels and reservoirs, can be created in paper sheets either by (i) the physical blocking of pores in the areas of the sheet external to the desired shape *via* patterning using a hydrophobic medium such as photoresist, ink, wax, PDMS, or other materials, or by (ii) cutting the paper sheet in the desired pattern using a craft cutter or laser cutter to create a stand-alone paper device in the desired shape.

Techniques for blocking of pores external to the patterned device, corresponding to (i) above, include photolithography,[1,23,24] ink jet printing,[25,26] plasma treatment,[27] screen printing,[28] chemical vapor deposition (CVD),[29] wax printing,[30,31] laser treatment,[32] and flexographic printing.[33,34] Of these, the most commonly used fabrication

[a] *Division of Engineering, New York University Abu Dhabi, Abu Dhabi, P.O. Box 129188, United Arab Emirates. E-mail: nk67@nyu.edu*
[b] *Department of Mechanical Engineering, New York University, Brooklyn, NY 11201, USA*

method is wax printing/dipping because of the low cost patterning material and promising potential in terms of rapid prototyping. However wax printing techniques have a set of challenges associated with them such as inconsistent patterning/reproducibility, issues with long term storage without climate control and instability at high temperatures, making them unsuitable for automated mass fabrication and storage.[35–38] Inkjet printers and laser toner printers provide another alternative for high throughput printing of hydrophobic barriers on paper substrates.[37,39,40] However, microPADs fabricated by using printers need an additional step of high temperature melting of toner ink to be impregnated into the paper matrix which may cause pyrolysis of cellulose and uses volatile organic solvents.[37,41] Flexographic printing is fast and well established for the fabrication of microPADs, but printing plates are expensive and changing plates for the printing of different designs is time consuming.[37,38] While techniques such as photolithography, CVD, and plasma treatment produce highly reproducible microPADs with good precision,[38,42,43] these methods are not cost-effective since they involve sophisticated equipment and procedures.[38,42,44]

Techniques to cut paper sheets into stand-alone devices, corresponding to (ii) described above, include using handheld and automated tools such as craft cutters or scissors, and computer controlled knives and lasers.[45–52] Some researchers have used cover tape/lamination tape to enclose open channels and hold individually cut devices to provide support and improve handling and functionality.[49–53] One of the ways that this is accomplished is by creating a hollowed mold of the same shape as the device in a lamination sheet or in Parafilm infused hardened paper, and inserting the paper device in the matched hollow receptacle.[50] Another is to use pieces of cover tape that have holes for ports for fluid access to the paper device.[51] Another technique places the individual devices under an opening of the same shape in a lamination sheet, but the opening is of slightly smaller dimensions which allows the edges of the paper device to be held by the periphery of the opening cut in the lamination sheet.[52] These techniques are labor intensive, require manual precision, and cannot be easily automated.

In the current study, a low-cost, simple and robust process is developed for the fabrication of microPADs using lamination sheets for the barrier formation making use of ethylene vinyl acetate (EVA), a hot melt adhesive, coated inside of the lamination sheets. Previously also, lamination sheets have been used for microPAD fabrication as holders or support for individually cut paper devices or for encapsulation, but not for device fabrication or being an integral part of the hydrophobic barriers.[49,50,53–55] The current fabrication process presents many key distinct advantages as compared to commonly used fabrication techniques discussed above. It is a two-step process, involving cutting of microfluidic patterns in the lamination sheets and heating them with a paper sheet in between them for the fabrication of microPADs, which thus are named as "cut and heat microPADs" (CH-microPADs). The fabricated devices as described here are highly robust against many chemicals such as strong acids, bases and solvents and possess very high mechanical strength against bending, folding, twisting and tearing, making them virtually unbreakable. The fabrication process involves minimal human intervention, making it ideally suitable for mass fabrication of microPADs in a large array for cut and use applications.

Experimental

Materials

Stationery purpose lamination sheets (typically available as office supplies and commonly used for the safety and protection of paper sheets) were used to create hydrophobic barriers on various types of cloth sheets such as cotton, polyester, and silk and paper sheets such as tissue paper, printing paper and filter paper. The commercially available lamination sheets are inexpensive and readily available from stationery stores. The lamination pouches are made of a polyethylene terephthalate (PET) outer layer and EVA inner layer.[56,57] Previously, researchers have used lamination sheets for covering open channels to minimize the evaporation of analytes and for providing mechanical support to the physically cut microPADs using a craft cutter and laser cutter.[51,58] EVA is a block-copolymer made by combining ethylene and vinyl acetate. EVA melting temperatures vary between 90 °C and 120 °C depending on the ratio of vinyl acetate and ethylene.[59] EVA copolymers are commonly used as hot-melt adhesives for various applications such as footwear, furniture, packaging, product assembly, book-binding and heat sealing applications.[60,61] A filter paper sheet, P8 grade (Fisherbrand) filter paper for the current studies or the paper sheet of interest, was then placed in between cut lamination sheets forming a sandwich structure (Fig. 1).

Device characterization: microscopy imaging

The paper devices, lamination sheet and paper sheets were imaged using an optical microscope (Nikon Eclipse LV100NDA). The device cross-sections were imaged to visualize the layered structure of lamination sheets with and without a paper sheet before and after heating (Fig. 2). The cross-sections were prepared by cutting the sheets using scissors. The images were obtained by mounting the cut cross-sections on a clamp and placing them under the microscope objective. The clamp kept the cross-section pieces in stable position under the objective while imaging.

Device characterization: SEM imaging

The surface and cross-sectional topography of the filter paper sheet and fabricated devices were observed using a scanning electron microscope (the Quanta 450 FEG, field emission

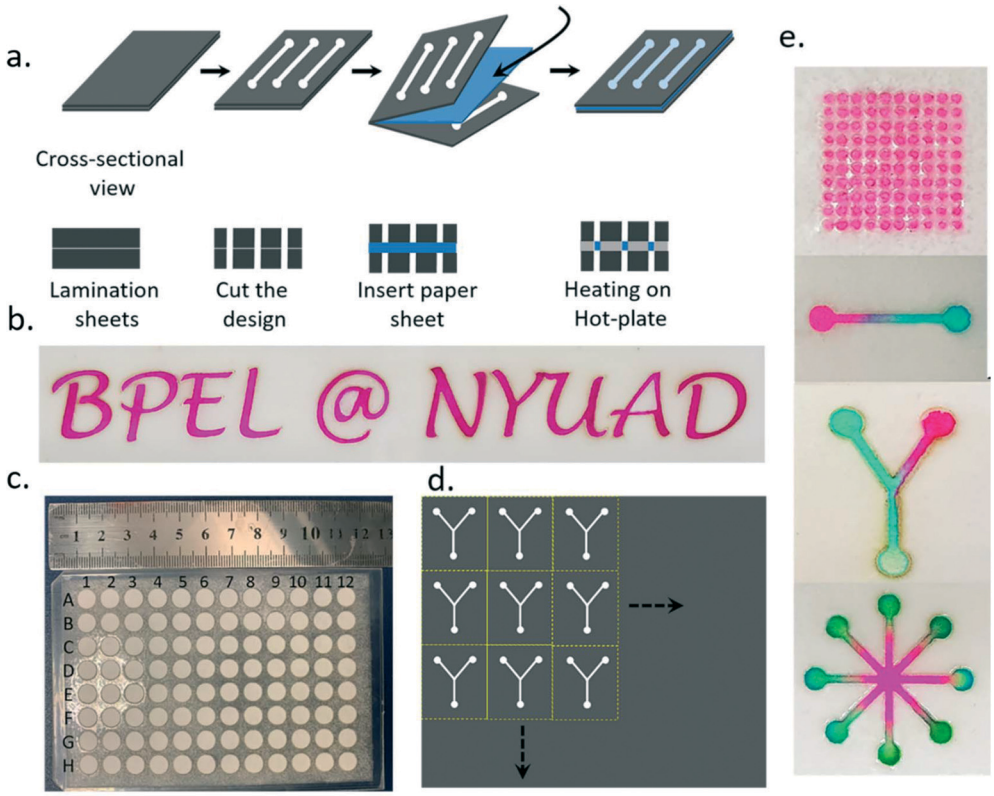

Fig. 1 Fabrication of CH-microPADs. (a) Schematic illustration of CH-microPAD assembly. It is a simple two-step process: first, cut the required device shapes in a pair of lamination sheets with the inner EVA sides facing each other and the PET sides outside on a laser cutter and then heat them on a hot plate with a paper sheet in between them. In the process of heating, EVA on the lamination sheets slowly melts and is impregnated into the paper sheet. The impregnated EVA forms hydrophobic barriers on the paper and leaves hydrophilic channels in the cut area on the lamination sheets. (b) Lab name; the letters were patterned on a qualitative grade plain filter paper sheet; rhodamine B was used as an analyte in the hydrophilic patterned area. (c) Top view of the fabricated 96 well plate showing the device dimensions and appearance. (d) Schematic showing the scalability of the proposed device fabrication process. Multiple devices can be fabricated in the form of an array on an A2/A3/A4 or A5 sheet and cut along the dotted line and used as needed at the point of need. (e) Various device designs fabricated using the proposed technique (top to bottom): micro array showing red color in the 800 micrometer circular hydrophilic wells, line, Y, and flower shapes showing the mixing of red and green colors to generate a yellow color after mixing.

scanning electron microscope (FE-SEM)). 700 ± 50 μm channel width devices were fabricated and imaged before and after heating (Fig. 3). The paper devices were coated with a thin 10 nm gold layer before imaging to increase the current conduction and reduce the charging effect.

Biological assays on CH-microPADs: cytocompatibility and cell viability assays

To evaluate the cytocompatibility and viability, mice embryonic fibroblasts (MEFs) were cultured on sterile CH-microPADs cut in the shape and dimensions of a traditional 96 well plate (Fig. 1c). In these, an additional laminating layer was introduced to cover the wells from the bottom side, which in turn helped to store the media for cell growth. The cell viability and growth were analyzed at 24, 48 and 72 hours. The CH-microPADs with cells and without cells were stained with live–dead assay reagents and imaged on a confocal microscope and assessed using ImageJ software. The stained cells on CH-microPADs showed remarkably enlarged green fluorescent colony formation by 72 hours compared to the 24 hours culture, while the red fluorescence intensity of cells was lower compared to the green one as observed at 72 hours, indicating cell compatibility, viability and growth on the CH-microPADs.

MTT assay for proliferation

The 3-(4,5-dimethylthiazol-2-yl)-2,5-diphenyl-2*H*-tetrazolium bromide (MTT) assay was used to test the metabolic activity of cells on the CH-microPADs fabricated in the form of a 96 well plate. The cell metabolic activity indicated the proliferation of cells at different time points of 24, 48 and 72 hours (Fig. 6). The MTT assay showed highly significant ($*p < 0.00001$) cell proliferation at 48 hours and 72 hours compared to that at 24 hours. At 72 hours, the MEF proliferation in the CH-microPADs exceeded that in the 2D monolayer culture, clearly indicating their potential use as a preferable material for 3D cell culture. The data showed here represent the mean and standard deviation of three

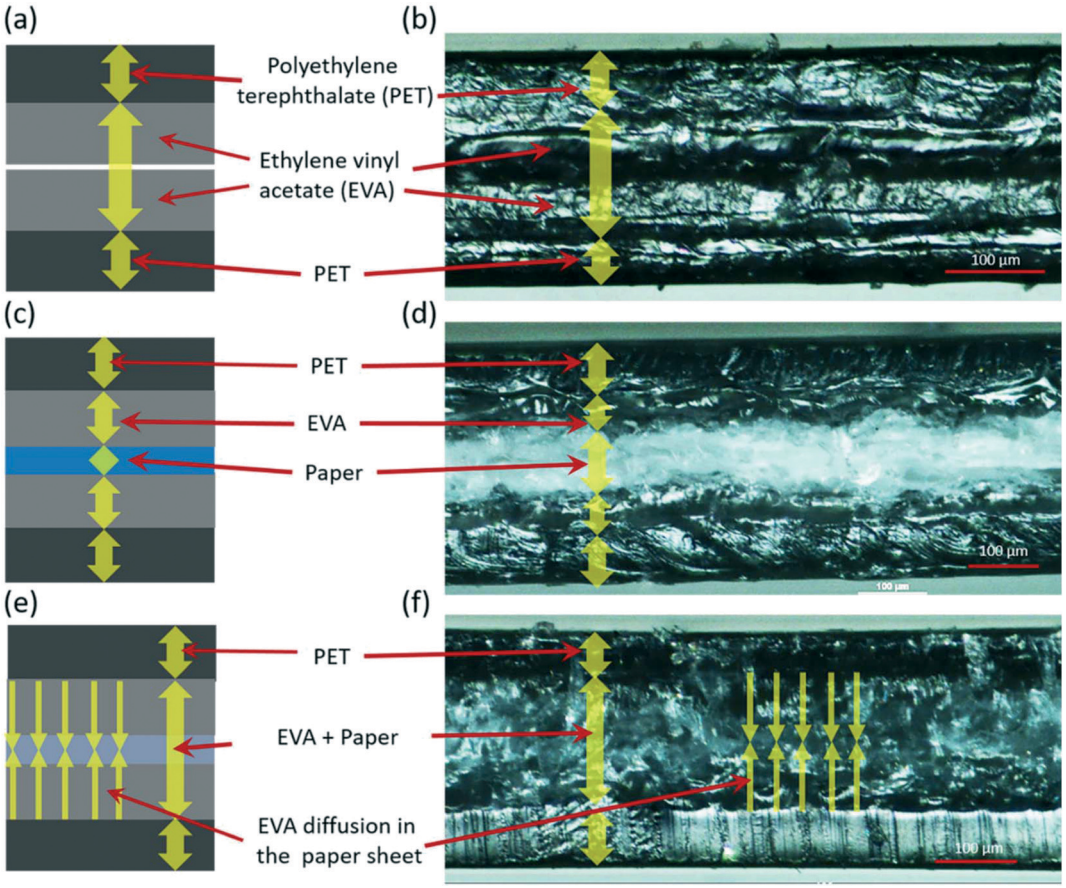

Fig. 2 EVA diffusion in the paper sheets while heating on a hot plate. (a) Schematic cross-sectional view of lamination sheets without paper, unheated, and (b) microscopy image of the cross-section of lamination sheets showing the PET and EVA layers separately. (c) and (d) Schematic cross-sectional view of lamination sheets with a paper sheet in between them and the corresponding microscopy image after 20 seconds of heating at 160 °C. (e) and (f) Schematic and microscopy images of the lamination sheets with a paper sheet in between them after 35 minutes of heating at 160 °C. It can be seen clearly from (e) and (f) that the EVA layer diffused completely in the paper sheet during the heating process, creating a hydrophobic barrier.

independent experiments in triplicate. The data were analyzed using two tailed Student's *t* test compared to the controls and the *p* values were calculated.

Immuno-detection assays

Direct ELISA was carried out to test the immuno-detection ability of the fabricated CH-microPADs in 96 well format (Fig. 7). IgG from rabbit serum, anti-rabbit IgG antibodies produced in goat (goat anti-rabbit IgG), anti-rabbit IgG–alkaline phosphatase conjugates (goat anti-rabbit IgG–ALP), and a 5-bromo-4-chloro-3-indolyl phosphate/nitroblue tetrazolium (BCIP/NBT) liquid substrate system were purchased from Sigma-Aldrich. Phosphate buffered saline (PBS) was obtained from Thermo Fisher Scientific. All reagents were used as received and sterile nuclease free water was used throughout the experiments. For detecting the dilution linearity of the ELISA reaction, rabbit IgG concentrations ranging from 0.01–1000 μg mL^{-1} were used. The rabbit IgG concentration which showed the most linear reaction kinetics was used for the actual ELISA experiments. Concentrations ranging from 1 μg mL^{-1} to 100 μg mL^{-1} were coated onto each well of the CH-microPADs in serial dilution and incubated for 12 hours at 4 °C. After incubation, the coated CH-microPAD wells were blocked with 1% BSA in PBS for one hour at room temperature, and then washed with PBS, and goat anti-rabbit IgG–alkaline phosphatase conjugates were added in a 1 : 200 dilution for one hour at room temperature. The enzymatic reactions were developed with the NBT–BCIP substrate for 15 minutes at room temperature.[62,63] All fluid volumes used were 10 μL per well. For quantifying the color development, CH-microPADs were analyzed on a BioTek microplate reader at an absorbance of 570 nm. A graph was plotted based on the mean color intensity after subtracting the blank well values. An iPhone camera (iPhone 10 XS Max, 12 megapixels) was used to capture the images of colorimetric assays as viewed with the naked eye. A Ricoh scanner was used to scan the color developed on the CH-microPADs at a resolution of 300 dpi after removing the liquid. The experiments were carried out at least three times in triplicate and analyzed statistically.

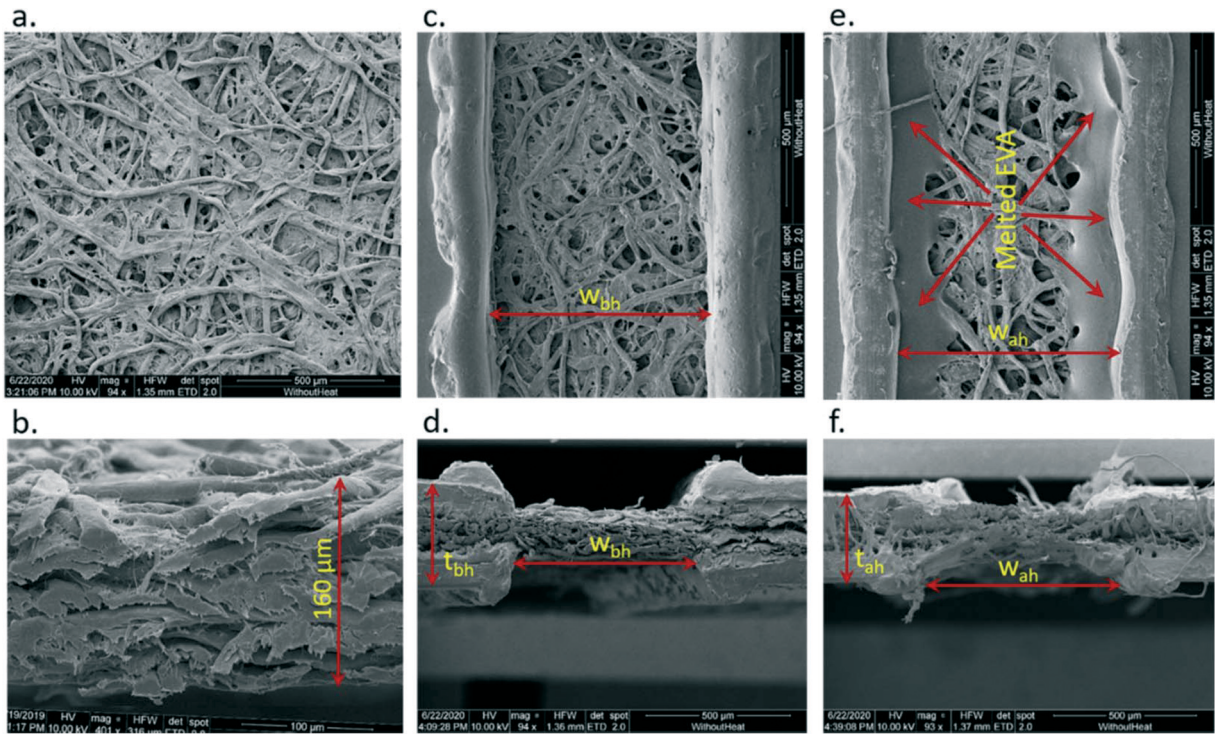

Fig. 3 SEM image of paper sheet and CH-microPAD before and after heating. (a) Top view of the porous paper sheet made of cellulose fibers. (b) Cross-sectional view of the paper sheet made of layers of cellulose fibers; the thickness of the paper sheet is approximately 160 μm. (c) Paper sheet sandwiched between lamination sheets having a 700 ± 50 μm wide channel cut in them; the device was heated for 20 seconds at 160 °C just to hold the paper sheet; w_{bh} = 700 ± 50 μm is the width of the channel before heating. (d) Cross-sectional view of the device in (c), showing open and sandwiched paper regions where t_{bh} = 360 μm was the thickness before heating of the sandwiched region. (e) The paper sandwich device in (c) was heated on a hot plate for 35 minutes at a temperature of 160 °C to make the sandwiched area hydrophobic and leave the open paper area hydrophilic. As the device got heated, EVA melted and diffused in the porous paper sheet vertically and laterally in the device channel near the channel walls. (f) Cross-sectional view of the device in (e), showing the device thickness t_{ah} = 310 μm and channel width after heating w_{ah} = 600 ± 50 μm. The device thickness and channel width decreased after heating as EVA diffused vertically in the paper sheet and laterally in the channel region.

Results

Design, cutting and fabrication of paper devices

The paper devices were designed in SolidWorks and exported to the .dxf format. Adobe Illustrator was used to open/edit and as an interface to give the print command to cut the devices. The device shapes were then cut using a multipurpose commercial laser cutter Epilog Laser Fusion 120 watts, used primarily for cutting and engraving of plastic and wood laminates. We used a laser power of 3 percent, and speed of 10 percent. These numbers were obtained after several iterations on plastic and paper sheets. Stationery purpose lamination sheets were used to create hydrophobic barriers on various types of cloth sheets such as cotton, polyester and silk and paper sheets such as tissue paper, printing paper and filter paper. A6, A5 and A4 size lamination pouches were used to cut the devices. Different sized lamination pouches (brand name MODEST from Modern Stationery LLC) were sourced from Amazon UAE. The lamination pouches can be of any other brand as well. The thickness of the lamination pouch (2 layers) was 250 μm. A filter paper sheet, or the paper sheet of interest, was then placed in between cut lamination sheets, Fig. 1a, forming a sandwich structure. The sandwich structures were then heated on a laboratory hot plate (IKA C-MAG HS 7), at different temperatures for varying durations.

Fabrication of paper devices

The CH-microPAD fabrication is a simple two-step process. In the first step, the devices were cut in a specific design in the lamination sheets and, in the second step, heated on a hot plate with a sheet of paper in between two lamination sheets having cut channels. The lamination sheets are typically polyethylene terephthalate (PET) sheets coated with ethylene vinyl acetate (EVA), which is a hot melt adhesive. For the device fabrication, the devices were designed in SolidWorks as per the needs of the experiments, for example in a single line, Y, circular array, or flower shape, or a 96 well plate format. The shapes were cut in the lamination sheets using a commercial laser cutter. The paper sheet was then placed in between cut lamination pouches (Fig. 1), forming a sandwich structure. The sandwich structures were then heated on a laboratory hot plate. When heated, the ethylene vinyl acetate (EVA) layer on the lamination sheets slowly melted and diffused in the paper sheet from the top and

bottom layers, shown schematically in Fig. 1a. The diffused EVA creates hydrophobic barriers and leaves cut areas as hydrophilic channels and sample/reaction spaces. In the uncut regions, melted EVA provides strong bonding of the lamination sheets to the paper. Using the process described, the letters 'BPEL @ NYUAD' were cut in the lamination sheets and used for patterning of hydrophilic and hydrophobic areas using a filter paper sheet. The patterned letters were used as hydrophilic regions to flow rhodamine B (which gives a pinkish color) as an analyte (Fig. 1b). The hydrophobic boundaries were strong and sharp (Fig. 1b), without any visible leak or blot at the ends.

The device designs can be cut in large numbers in A2, A3, A4 or A5 lamination sheets and then heated on a hot plate either one sheet at a time or in a stacked fashion. The individual microPADs then can be cut and used as needed from the mass fabricated array of CH-microPADs (Fig. 1d). The technique was used for the fabrication of different device designs such as a 96 well plate (Fig. 1c), circular array, line, Y and flower shape (Fig. 1e). The line, Y and flower shaped devices were shown for the mixing of red and green colors to generate a yellow color. These device designs can be used for various sensing and quality control applications based on mixing of analytes or reaction of analytes with the cells seeded in the hydrophilic inlet reservoirs. In the current study, we have used fabricated 96 well plates for cell culture applications and detection of proteins and enzymes using enzyme-linked immunoassay (ELISA) in the hydrophilic 3D porous paper matrix.

Hydrophobic barrier formation process

The cross-sectional view highlighting the layered structure of the lamination pouch consisting of PET and EVA layers is shown schematically in Fig. 2a and microscope image in Fig. 2b. A filter paper sheet was placed between two lamination sheets and heated for 20 seconds at 160 °C; the schematic of the corresponding cross-sectional view is shown in Fig. 2c and the microscope image in Fig. 2d. It can be observed that within 20 seconds, the EVA layer started melting and diffusing in the paper sheet, and in turn made firm contact with the paper sheet. After heating for 20 seconds at 160 °C, the thickness of the layered assembly was approximately 360 μm (Fig. 2d). As the filter paper sandwiched lamination sheets were heated for 35 minutes at 160 °C, the EVA layer diffused completely in the paper layer, changing the paper color from white to charcoal grey, matching with the color of the EVA layer (Fig. 2f). It can be observed from Fig. 2f that the thickness of the layered assembly was reduced to 310 μm as compared to 360 μm in Fig. 2d. The reduction in the thickness was due to the slow diffusion of the EVA layer in the porous filter paper as it was continually heated at 160 °C.

SEM imaging of paper and fabricated devices

The surface and cross-sectional topography of the filter paper sheet and fabricated devices were observed using a scanning electron microscope (SEM) before and after heating the devices. For the device fabrication, filter paper sheets were used, and SEM images of the surface and cross-sectional view of the paper sheet are shown in Fig. 3a and b. The paper sheet is made of multiple layers of cellulose fibers and the thickness of the paper sheet is approximately 160 micrometers (μm) (Fig. 3b). The paper sheet was placed between two lamination sheets having a channel of 700 ± 50 μm width and the sandwich assembly was heated for 20 seconds at 160 °C. The short 20 s heating was to hold it properly for imaging purposes only so that the paper sheet made good contact with the lamination sheets and did not move while handling the device. The channel top view and cross-section after 20 s heating are shown in Fig. 3c and d. The device was then heated at 160 °C for 35 minutes. With heating, the EVA diffused in the paper sheet in the vertical direction and also in the channel area laterally (Fig. 3e and f). On heating, the sandwiched area became hydrophobic because of the diffusion of melted EVA in the paper sheet and open paper areas remained hydrophilic for the flow of analytes.

Optical microscopy imaging of fabricated devices

Devices with the same specifications as those in Fig. 3 were also imaged under a microscope before and after heat treatment (Fig. 4). A 700 ± 50 micrometer (μm) width channel was cut in the lamination sheets and a filter paper sheet was placed in between them (Fig. 4a(i)). The top and cross-sectional view of the device before heating are shown in Fig. 4a(i) and (ii), respectively, highlighting the open paper region, which will be hydrophilic, and the sandwiched paper region between lamination sheets, which will become hydrophobic after heating the device structure. The device structure was then heated on a hot plate for 35 minutes at 160 °C. When heated at a temperature of 160 °C, the EVA layer, in contact with the paper sheet, slowly melted and diffused in the paper sheet. After heating, the sandwiched areas were seen brighter under the microscope compared to those before heating; this is because when EVA is diffused in the paper sheet, pores and blank areas in between fibers were filled with EVA, causing less light scattering and absorbing by the paper sheet (Fig. 4a(iii)). The cross-sectional view of the device structure after heating highlights that the color of paper sheet turned to charcoal grey from white as the EVA layer diffused in the paper sheet on heating (Fig. 4a(iv)). The sandwiched paper region turned to a hydrophobic region due to the diffused EVA and created sharp boundaries from the open hydrophilic paper region for confinement of liquids. When the hydrophilic paper region in the device was introduced with 5 microliters of rhodamine B, it showed a clear boundary between the colored paper region and hydrophobic sandwiched region (Fig. 4a(v)). The cross-sectional view of the device structure with rhodamine B is shown in Fig. 4a(vi). The EVA layer, when melted, diffused isotropically in the paper sheet both in the vertical and lateral directions, forcing it into the hydrophilic paper channel, as shown with dashed yellow lines in Fig. 4a. The isotropic flow of

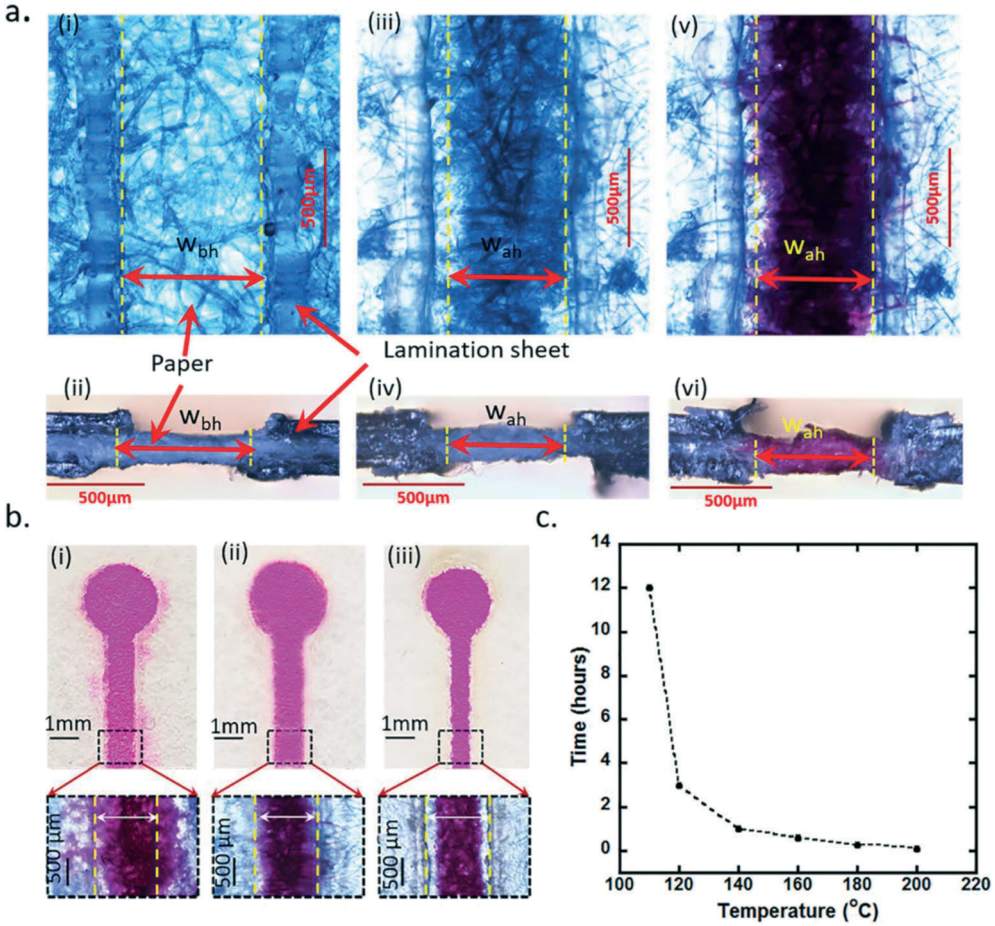

Fig. 4 Microfluidic channel shown under an optical microscope: a(i) heated for 20 seconds at 160 °C, a(iii) heated for 1 hour at 160 °C making the sandwiched area completely hydrophobic and leaving the open area hydrophilic, a(v) rhodamine B in the hydrophilic channel area, and a(ii), a(iv) and a(vi) cross-sections of the channel in a(i), a(iii) and a(v) respectively. (b) Effect of heating duration on fluid confinement. b(i) Image of the device showing leakage of rhodamine B; the heating for 20 minutes at 160 °C was insufficient to diffuse EVA in the paper sheet to make it completely hydrophobic outside of the channel regions. b(ii) The device, showing good confinement of rhodamine B in the channel region, after heating for 35 minutes at 160 °C. b(iii) Image of the device showing a reduced channel width because of overheating; it was heated for 60 minutes at 160 °C. The insets show the zoomed in images of the highlighted areas under the microscope. (c) Heating temperature *vs.* time taken for EVA to completely diffuse (vertically) in the paper sheet in the sandwiched paper area with minimal diffusion in the open channel regions.

EVA on heating reduced the effective channel width from 700 ± 50 μm (w_{bh}) to 600 ± 50 μm (w_{ah}) (Fig. 4a(iii) and (v) respectively).

The present technique overcomes difficulties faced by wax patterning to create hydrophobic barriers. The main limitation of wax based patterning is in achieving control of the flow of the melted wax while creating barriers in porous paper media.[30] Here, the present technique offers a simple two-step process having precise control to form hydrophobic barriers in which sandwiched regions became hydrophobic on heating whereas open areas were left hydrophilic. Another advantage is the very high thermal stability up to 100 °C offered by these devices. This is because the EVA diffusion process only starts at temperatures higher than 110 °C and it takes more than 12 hours even at 110 °C for the EVA to completely diffuse in the paper sheets. Therefore, the proposed CH-microPADs are ideally suited for high temperature analyte measurements as well.

The heating duration at a specific temperature is a very important parameter for uniform diffusion of EVA inside the paper sheets. The EVA needs to be diffused completely while heating through the paper sheet in order to make it completely hydrophobic. If the heating is uneven and has a shorter duration, the EVA diffusion will not be uniform, leaving hydrophilic parts in the sandwiched area. Three devices were tested to study the effect of heating duration on liquid confinement; the devices were heated at 160 °C for three different time durations. For the testing, 1 mm channel devices having a 2 mm diameter test area were fabricated. In each device, 5 microliters of rhodamine B was introduced to see its spread. The liquid confinement was different for all three devices as shown in the images of the devices with the insets showing zoomed in images of the areas highlighted under the microscope (Fig. 4b). Device 1 was heated for 20 minutes at 160 °C, and it can be observed that the dye leaked and spread out of the channel, making the effective width of

the channel more than 1 mm (Fig. 4b(i)). Device 2 was heated for 35 minutes at 160 °C. Rhodamine B remained confined within the channel width, and the effective channel width was 1 ± 0.05 mm measured under the microscope (Fig. 4b(ii)). The third device was heated for 60 minutes at 160 °C. With overheating, the EVA diffused deeper in the channel area resulting in a narrower channel, reducing the channel width from 1 mm to 0.750 ± 0.05 mm (Fig. 4b(iii)). Therefore, the heating at 160 °C for a duration of 35 minutes was found to be optimal; it resulted in leak-proof channels with sharp boundaries between the hydrophobic and hydrophilic areas.

The lower the temperature, the longer the heating duration should be for optimal EVA diffusion in the porous sheet and *vice versa*. In order to optimize the heating temperature and duration, the sandwich structures were heated at various temperatures such as 110 °C, 120 °C, 140 °C, 160 °C, 180 °C and 200 °C for different durations. It took 12 hours, 3 hours, 1 hour, 35 minutes, 15 minutes, and 5 minutes respectively to completely diffuse EVA through qualitative grade plain filter paper sheets – P8 grade (Fisherbrand). When different porous media such as cloth or other types of paper are used, the temperature *vs.* time duration has to be optimized. The heating process showed an inverse relationship with the heating duration (Fig. 4c). The process can be multiplexed by heating multiple device structures arranged in a stack.

Minimum channel width and stability of CH-microPADs against various chemicals

Channels of different widths ranging from 0.2 mm to 1 mm were fabricated to determine the minimum channel width of CH-microPADs. The channels were 10 mm in length with a 2 mm diameter reservoir at both ends (Fig. 5a). The sandwiched structures were heated at 160 °C for 35 minutes on a hot plate. In each device, 5 microliters of rhodamine B was introduced. All the devices showed the flow of rhodamine B from one end to the other end, except for the 0.2 mm device. The channel widths were measured under the microscope (Fig. 5b) and are shown as insets in Fig. 5a. A minimum channel width of 0.3 ± 0.05 mm was obtained

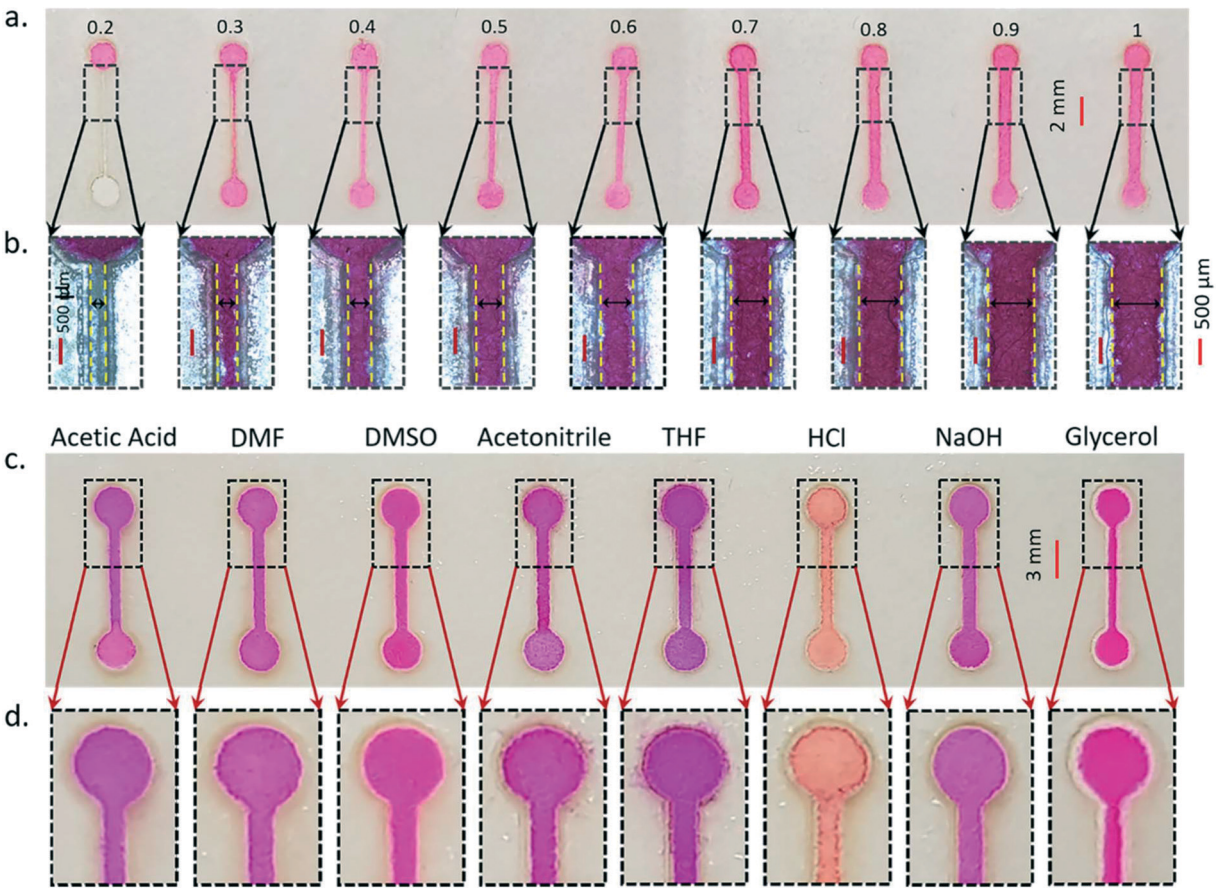

Fig. 5 Resolution of the CH-microPADs and chemical stability. (a) 0.3 ± 0.05 mm was the minimum channel width obtained with repeated device measurements (n = 10). The devices were fabricated with 2 mm reservoirs and channel widths ranging from 0.2 mm to 1 mm and a channel length of 10 mm. The devices were introduced with 5 microliters of rhodamine B at one end of the device for visual confirmation and size measurements. (b) Zoomed in areas from (a) under the microscope. (c) Flow of various acids, bases and solvents mixed with rhodamine B in a 1 mm wide and 10 mm long channel showing the stability of CH-microPADs. Acetonitrile and THF showed some leakage during the introduction in the inlet port, while the other chemicals showed very good stability. (d) Zoomed in areas from (c) at the inlet port.

for the CH-microPADs with repeated device measurements (n = 10).

In order to evaluate the chemical stability, the CH-microPADs were exposed to several chemicals such as acids, bases and solvents. For the testing, 1 mm wide and 10 mm long channels with a 3 mm diameter reservoir at both ends were fabricated (Fig. 5c). The EVA formed barriers were stable against most of the chemicals such as acetic acid, dimethylformamide (DMF), dimethyl sulfoxide (DMSO), hydrochloric acid (HCl), sodium hydroxide (NaOH) and glycerol. The chemicals were mixed with rhodamine B dissolved in water and introduced into the channel reservoir as shown in Fig. 5c. The concentration of HCl and NaOH was 1 M and the other chemicals were undiluted except glycerol (diluted at a ratio of 1 : 5 with deionized water). Acetonitrile and tetrahydrofuran (THF) showed some leakage at the introduction reservoir (Fig. 5d). It is significant to note that the barriers were resistant to most of the chemicals used including strong acids and bases. The CH-microPADs showed good chemical resistance to various solvents, acids and bases, showing the strong compatibility of the devices for a variety of solvents and analytes.

Biological assays: cytocompatibility and cell viability

Mice embryonic fibroblasts (MEFs – ATCC® CRL-2752) at a concentration of 0.01 × 10^6 were cultured on UV sterilized individual CH-microPADs, placed inside the wells of 96 well plates for 24, 48 and 72 hours and stained with calcein AM and ethidium homodimer 1 (Invitrogen LIVE/DEAD™ Viability/Cytotoxicity kit, for Mammalian Cells, L3224). Prior to staining, the cells were washed with prewarmed physiological saline. The cells in the CH-microPADs were stained with 100 μL of 2 M calcein AM and 4 M ethidium homodimer 1 working solution for 45 minutes at room temperature. After the incubation, the CH-microPADs were lifted from the wells and mounted on a clean slide followed by confocal imaging using a Leica SP8 confocal laser scanning microscope. In this staining method, live cells are distinguished by the presence of ubiquitous intracellular esterase activity, determined by the enzymatic conversion of the virtually nonfluorescent cell-permeant calcein AM to the intensely fluorescent calcein. The polyanionic dye calcein is well retained within live cells, producing an intense uniform green fluorescence in live cells. The ethidium homodimer 1 dye enters cells with damaged membranes and undergoes a 40-fold enhancement of fluorescence upon binding to nucleic acids, thereby producing a bright red fluorescence in dead cells. The results of the assay are displayed in Fig. 6a.

MTT assay for cell proliferation

The MTT assay was used to test for cell proliferation on the CH-microPADs. MEFs cultured on wells as monolayers were used as the control. The mechanism of this assay is based on metabolically active cells reducing the tetrazolium salt MTT (3-(4,5-dimethylthiazol-2-yl)-2,5-diphenyltetrazolium bromide) to purple formazan (MTT cell proliferation kit, catalogue number 11465007001, Roche). The CH-microPADs with a thickness of 120 μm and diameter of 6 mm were placed in each well of a 96 well plate inside a biosafety cabinet. The scaffolds were sterilized under UV radiation for one hour each on both sides. MEFs at a concentration of 0.01 × 10^6 cells per well were plated onto the CH-microPADs placed in each well. The plates were incubated at 37 °C with 5% CO_2 for one hour. After the incubation, 100 μL of DMEM containing 10% fetal bovine serum (FBS) and 1× antibiotics (Sigma) were added to each well, and incubated at 37 °C with

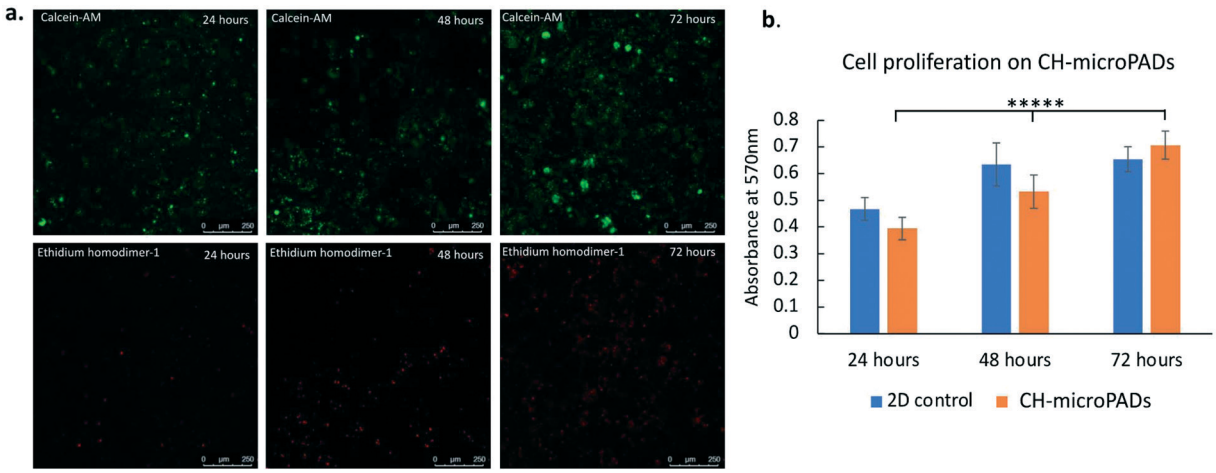

Fig. 6 Cell compatibility and proliferation on CH-microPADs: the CH-microPADs showed excellent biocompatibility characteristics while culturing mouse embryonic fibroblasts (MEFs) in 96 well format culture vessels. The cell viability and proliferation were analyzed by live–dead staining and the MTT assay at 24, 48 and 72 hours. (a) The live–dead staining showed remarkably enlarged green fluorescent (live cells) colonies at 72 h compared to those at 24 h. The red fluorescence (dead cells) intensity of cells was lower compared to the green one as observed at 72 h, indicating excellent cell compatibility and viability. (b) The MTT assay showed significant (*****$p < 0.00001$) cell proliferation on CH-microPADs at 48 hours and 72 hours compared to that at 24 hours.

5% CO_2 for three time points, 24 hours, 48 hours, and 72 hours. The growth of the MEF colonies was imaged at these time points on a confocal microscope and assessed using ImageJ (Fig. 6a). At each time point, 10 μl MTT labelling solution was added to each well followed by incubation for 4 hours. After 4 hours, 100 μL MTT solubilization reagent was added to each well and incubated overnight. Media without cells and with the CH-microPADs were used as blank. A 2D monolayer MEF culture was used as cell growth control. 100 μL aliquots from culture wells were transferred to another 96-well plate for measuring absorbance. Absorbance was measured at a wavelength of 570 nm using a microplate reader (Epoch, BioTek). All steps in the MTT assays were conducted in the dark as the MTT assay reagents are sensitive to light. The results of the assay are depicted in Fig. 6b.

ELISA based immuno-detection assay on CH-microPADs

A proof-of-concept design of enzyme based immuno-detection using the fabricated CH-microPADs (in a 96 well plate format as shown in Fig. 1c) was explored. Rabbit IgG in serial dilution was coated onto each well of the CH-microPADs and detected using goat anti-rabbit IgG–alkaline phosphatase conjugates. The enzymatic reaction of the antibody conjugated alkaline phosphatase was developed with the nitroblue tetrazolium (NBT)–5-bromo-4-chloro-3-indolyl phosphate (BCIP) substrate. The enzymatic reaction observed was directly proportional to the concentration of rabbit IgG coated onto the wells. The wells coated with 100 μg mL^{-1} rabbit IgG showed maximum color development while the lower concentration IgG coated wells showed a less intense color in a serial manner. Fig. 7 shows the assay scheme and the result of the enzymatic immuno-detection on CH-microPADs.

Discussion

MicroPADs are lightweight, disposable, low-cost point of care devices with simple fabrication and ease of operation. They enable fluid transport *via* capillary action due to the hydrophilic and porous nature of paper, without the need of external pumps and a power supply, as compared to microfluidic devices made with glass, silicon, and/or polymers. Many techniques have been demonstrated for the patterning of paper sheets based on ink jet printing,[25,26] screen-printing,[28] photolithography,[1,23,24] plasma treatment,[27] CVD,[29] wax printing,[30,31] flexographic printing,[33] laser treatment[32] and techniques based on automated/handheld tools.[34,45–48] Even after a decade and a half since their first introduction in 2007, the successful commercialization and scale-up of microPADs has remained a challenge. This is primarily because of challenges associated with many of these techniques for the automated mass fabrication of microPADs. Wax printing is commonly used for the patterning of channel barriers on a paper sheet; however wax printers are not commonly available. Patterning with wax also poses challenges related to flow control and leakage problems with surfactant mixed biological samples.[36] While techniques such as CVD, photolithography and plasma treatment provide good reproducibility and precision, they involve complex processing steps to be carried out under specific laboratory conditions which in turn increases the cost of the microPADs.[64] The microPADs fabricated by the techniques mentioned above also lack good mechanical robustness as compared to conventional microfluidic devices made from polymers, glass and/or silicon.[65] A promising technique for practical applications in both resource-limited settings and developed ecosystems should be suitable for mass fabrication with minimal fabrication steps, low cost, good mechanical strength and high precision and reproducibility.

In the current work, a two-step process for the selective fabrication of hydrophilic channels and reservoirs on a

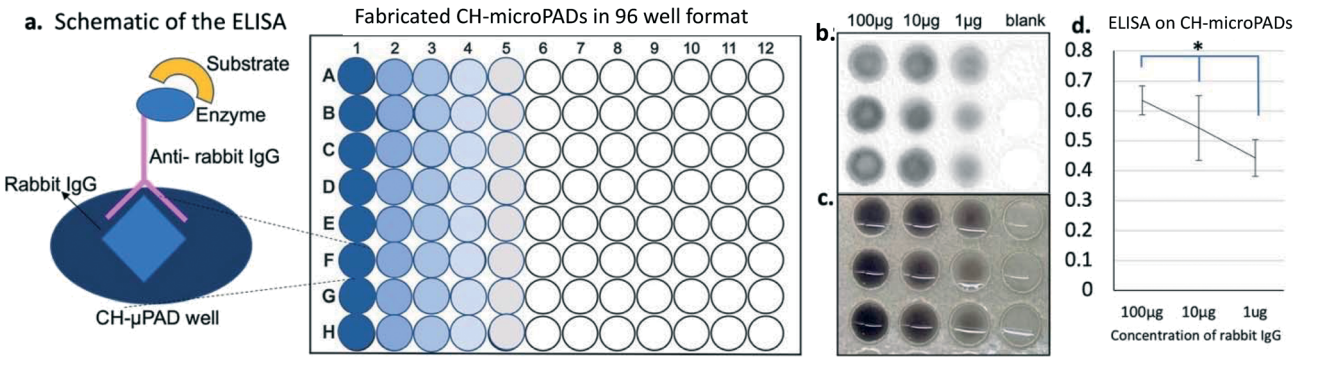

Fig. 7 Direct ELISA based immuno-detection on CH-microPADs: (a) the schematic representation of the ELISA on the CH-microPADs. The colorimetric signal is based on the concentration of rabbit IgG coated on the fabricated CH-microPAD microwells. (b) Scanned image of the ELISA reaction on the CH-microPADs. (c) The image of the color development captured using an iPhone camera. (d) The graph plotted based on the colorimetric reaction analysis using a microplate reader. The color development was directly proportional to the concentration of rabbit IgG coated on the well. The result was statistically significant (*$p < 0.05$) between each concentration tested.

porous sheet is demonstrated for the fabrication of microPADs in various designs. The process can be used to create hydrophobic barriers on a wide variety of porous media such as tissue paper, printing paper, and filter paper and a wide variety of cloth types such as cotton, silk and polyester. MicroPADs are fabricated only by using widely commercially available lamination pouches and filter paper or any porous media of interest as a consumable material, making it widespread. Previously, lamination sheets in the literature have been used as support for individually cut paper devices or for encapsulation or to function as holders, but not for device fabrication nor as an integral part of hydrophobic barriers, as presented in the present technique. The technique presented here overcomes the many challenges associated with the current techniques shown in the literature. The fabricated 96 well plate CH-microPADs were tested for cell culture and protein and enzyme detection in the ELISA format.

In vitro biocompatibility and cell proliferation assays using MEFs on fabricated CH-microPADs in the form of 96 well plates showed good cytocompatibility and cell proliferation. Cell-incorporated CH-microPADs can be developed into an easily maintainable 3D cell culture system to be used in tissue transplants such as skin patches for burn injuries and wound care.[66] The cellulose material used to make the CH-microPADs is biocompatible, nontoxic and environment friendly. Also, as a future study, different growth modulators, silver nanoparticles and drug molecules can be incorporated in the CH-microPADs along with cellular components to translate this research into clinical application. The protein adsorption capacity of the fabricated CH-microPADs appeared consistent in the ELISA experiments. The amount of reagents required to do the assay is 5–10 μL in each step, which saves costly immuno-detection reagents compared to the traditional 96 well plate plastics. This observation expands its scope to be used as an immunodiagnostic device. Current paper based immuno-detection devices are mostly limited to test strip-based applications. But, amidst global pandemic crises such as COVID-19, it is essential to develop efficient and cheaper mass diagnostic devices. 96 or 386 well format CH-microPADs would be useful to bring in huge improvements in the immunoassay throughputs at mass point-of-care testing units. The proposed CH-microPADs are cheaper to produce, can be stored in less space at room temperature, and can reduce the use of expensive immune reagents and polluting plastic materials per immunoassay.

Conclusion

In this study, an affordable, simple and easily accessible technique is developed for rapid fabrication of low-cost microPADs. The fabrication process can be used to create any device designs or fluidic patterns on porous sheets. The device shapes and designs are cut using a commercial laser cutter, making the process robust and repeatable every time, unlike many other techniques used to fabricate microPADs where repeatability is a major concern. The fabrication steps involve minimal human intervention, making the process ideal for automation, which is a key feature aimed at mass fabrication of CH-microPADs. The devices can be made in an array on A2/A3/A4 or A5 sheet sizes and be cut and used as needed at the point of need. The fabrication process was characterized and demonstrated by creating different device designs on various types of paper and cloth sheets. The presented technique circumvents the use of clean room facilities and harsh chemicals making it easily accessible for point of use fabrication of microPADs. The fabricated devices are highly robust and chemically stable for a wide range of solvents, strong acids and bases. Moreover, the devices possess very high mechanical strength against bending, folding, twisting and tearing. The fabricated devices are virtually unbreakable since the devices are fabricated through a lamination process commonly used for the protection of paper sheets. In summary, a simple, low-cost and robust rapid prototyping technique is demonstrated for the fabrication of CH-microPADs for biological and healthcare applications. The simplicity and versatility of the fabrication process demonstrated will lead to its widespread adoption in both resource-limited and developed settings.

Conflicts of interest

There are no conflicts to declare.

Acknowledgements

We thank Mr. Vijay Dhanvi, and acknowledge the technical support from the Core Technology Platforms at NYU Abu Dhabi.

References

1 A. W. Martinez, *et al.*, Patterned Paper as a Platform for Inexpensive, Low-Volume, Portable Bioassays, *Angew. Chem., Int. Ed.*, 2007, **46**(8), 1318–1320.
2 A. W. Martinez, *et al.*, Simple Telemedicine for Developing Regions: Camera Phones and Paper-Based Microfluidic Devices for Real-Time, Off-Site Diagnosis, *Anal. Chem.*, 2008, **80**(10), 3699–3707.
3 V. Oncescu, D. O'Dell and D. Erickson, Smartphone based health accessory for colorimetric detection of biomarkers in sweat and saliva, *Lab Chip*, 2013, **13**(16), 3232–3238.
4 A. A. Kumar, *et al.*, From the Bench to the Field in Low-Cost Diagnostics: Two Case Studies, *Angew. Chem., Int. Ed.*, 2015, **54**(20), 5836–5853.
5 M. M. Gong and D. Sinton, Turning the Page: Advancing Paper-Based Microfluidics for Broad Diagnostic Application, *Chem. Rev.*, 2017, **117**(12), 8447–8480.
6 J. R. Choi, *et al.*, Emerging Point-of-care Technologies for Food Safety Analysis, *Sensors*, 2019, **19**(4), 817.
7 S. Chaiyo, *et al.*, Highly selective and sensitive paper-based colorimetric sensor using thiosulfate catalytic etching of silver nanoplates for trace determination of copper ions, *Anal. Chim. Acta*, 2015, **866**, 75–83.

8 J. R. Choi, *et al.*, An integrated paper-based sample-to-answer biosensor for nucleic acid testing at the point of care, *Lab Chip*, 2016, **16**(3), 611–621.
9 C.-C. Liu, *et al.*, Microfluidic paper-based chip platform for benzoic acid detection in food, *Food Chem.*, 2018, **249**, 162–167.
10 Y. Zhang, P. Zuo and B.-C. Ye, A low-cost and simple paper-based microfluidic device for simultaneous multiplex determination of different types of chemical contaminants in food, *Biosens. Bioelectron.*, 2015, **68**, 14–19.
11 S. S. Nadar, *et al.*, Enzyme embedded microfluidic paper-based analytic device (μPAD): a comprehensive review, *Crit. Rev. Biotechnol.*, 2021, **41**(7), 1046–1080.
12 Y. Chen, *et al.*, Point-of-care and visual detection of P. aeruginosa and its toxin genes by multiple LAMP and lateral flow nucleic acid biosensor, *Biosens. Bioelectron.*, 2016, **81**, 317–323.
13 B. Li, *et al.*, Quantum Dot-Based Molecularly Imprinted Polymers on Three-Dimensional Origami Paper Microfluidic Chip for Fluorescence Detection of Phycocyanin, *ACS Sens.*, 2017, **2**(2), 243–250.
14 P. Wang, *et al.*, Development of a paper-based, inexpensive, and disposable electrochemical sensing platform for nitrite detection, *Electrochem. Commun.*, 2017, **81**, 74–78.
15 C. Sicard, *et al.*, Tools for water quality monitoring and mapping using paper-based sensors and cell phones, *Water Res.*, 2015, **70**, 360–369.
16 F. F. Tao, *et al.*, Paper-based cell culture microfluidic system, *BioChip J.*, 2015, **9**(2), 97–104.
17 B. Hong, *et al.*, A concentration gradient generator on a paper-based microfluidic chip coupled with cell culture microarray for high-throughput drug screening, *Biomed. Microdevices*, 2016, **18**(1), 21.
18 G. Musile, *et al.*, The development of paper microfluidic devices for presumptive drug detection, *Anal. Methods*, 2015, **7**(19), 8025–8033.
19 A. W. Martinez, *et al.*, Diagnostics for the Developing World: Microfluidic Paper-Based Analytical Devices, *Anal. Chem.*, 2010, **82**(1), 3–10.
20 N. Z. Piety, *et al.*, A Paper-Based Test for Screening Newborns for Sickle Cell Disease, *Sci. Rep.*, 2017, **7**(1), 45488.
21 M. S. Hede, *et al.*, Detection of the Malaria causing Plasmodium Parasite in Saliva from Infected Patients using Topoisomerase I Activity as a Biomarker, *Sci. Rep.*, 2018, **8**(1), 4122.
22 L. Magro, *et al.*, Paper-based RNA detection and multiplexed analysis for Ebola virus diagnostics, *Sci. Rep.*, 2017, **7**(1), 1347.
23 A. W. Martinez, S. T. Phillips and G. M. Whitesides, Three-dimensional microfluidic devices fabricated in layered paper and tape, *Proc. Natl. Acad. Sci. U. S. A.*, 2008, **105**(50), 19606.
24 S. A. Klasner, *et al.*, Paper-based microfluidic devices for analysis of clinically relevant analytes present in urine and saliva, *Anal. Bioanal. Chem.*, 2010, **397**(5), 1821–1829.
25 K. Abe, K. Suzuki and D. Citterio, Inkjet-Printed Microfluidic Multianalyte Chemical Sensing Paper, *Anal. Chem.*, 2008, **80**(18), 6928–6934.
26 K. Abe, *et al.*, Inkjet-printed paperfluidic immuno-chemical sensing device, *Anal. Bioanal. Chem.*, 2010, **398**(2), 885–893.
27 X. Li, *et al.*, Paper-Based Microfluidic Devices by Plasma Treatment, *Anal. Chem.*, 2008, **80**(23), 9131–9134.
28 W. Dungchai, O. Chailapakul and C. S. Henry, A low-cost, simple, and rapid fabrication method for paper-based microfluidics using wax screen-printing, *Analyst*, 2011, **136**(1), 77–82.
29 T. Lam, *et al.*, A Chemically Patterned Microfluidic Paper-based Analytical Device (C-μPAD) for Point-of-Care Diagnostics, *Sci. Rep.*, 2017, **7**(1), 1188.
30 E. Carrilho, A. W. Martinez and G. M. Whitesides, Understanding Wax Printing: A Simple Micropatterning Process for Paper-Based Microfluidics, *Anal. Chem.*, 2009, **81**(16), 7091–7095.
31 Y. Lu, *et al.*, Fabrication and Characterization of Paper-Based Microfluidics Prepared in Nitrocellulose Membrane By Wax Printing, *Anal. Chem.*, 2010, **82**(1), 329–335.
32 G. Chitnis, *et al.*, Laser-treated hydrophobic paper: an inexpensive microfluidic platform, *Lab Chip*, 2011, **11**(6), 1161–1165.
33 J. Olkkonen, K. Lehtinen and T. Erho, Flexographically Printed Fluidic Structures in Paper, *Anal. Chem.*, 2010, **82**(24), 10246–10250.
34 P. de Tarso Garcia, *et al.*, A handheld stamping process to fabricate microfluidic paper-based analytical devices with chemically modified surface for clinical assays, *RSC Adv.*, 2014, **4**(71), 37637–37644.
35 A. K. Yetisen, M. S. Akram and C. R. Lowe, Paper-based microfluidic point-of-care diagnostic devices, *Lab Chip*, 2013, **13**(12), 2210–2251.
36 X. Li, D. R. Ballerini and W. Shen, A perspective on paper-based microfluidics: Current status and future trends, *Biomicrofluidics*, 2012, **6**(1), 011301.
37 M. S. Khan, S. A. Shadman and M. M. R. Khandaker, Advances and current trend of bioactive papers and paper diagnostics for health and biotechnological applications, *Curr. Opin. Chem. Eng.*, 2022, **35**, 100733.
38 Z. Hao, *et al.*, Fabrication for paper-based microfluidic analytical devices and saliva analysis application, *Microfluid. Nanofluid.*, 2021, **25**(10), 80.
39 K. Yamada, *et al.*, Paper-Based Inkjet-Printed Microfluidic Analytical Devices, *Angew. Chem., Int. Ed.*, 2015, **54**(18), 5294–5310.
40 A. Apilux, *et al.*, Development of automated paper-based devices for sequential multistep sandwich enzyme-linked immunosorbent assays using inkjet printing, *Lab Chip*, 2013, **13**(1), 126–135.
41 J. S. Ng and M. Hashimoto, Fabrication of paper microfluidic devices using a toner laser printer, *RSC Adv.*, 2020, **10**(50), 29797–29807.
42 T. Akyazi, L. Basabe-Desmonts and F. Benito-Lopez, Review on microfluidic paper-based analytical devices towards commercialisation, *Anal. Chim. Acta*, 2018, **1001**, 1–17.
43 E. Noviana, *et al.*, Microfluidic Paper-Based Analytical Devices: From Design to Applications, *Chem. Rev.*, 2021, **121**(19), 11835–11885.

44 D. M. Cate, *et al.*, Recent Developments in Paper-Based Microfluidic Devices, *Anal. Chem.*, 2015, **87**(1), 19–41.
45 E. M. Fenton, *et al.*, Multiplex Lateral-Flow Test Strips Fabricated by Two-Dimensional Shaping, *ACS Appl. Mater. Interfaces*, 2009, **1**(1), 124–129.
46 W. Wang, *et al.*, Tree-shaped paper strip for semiquantitative colorimetric detection of protein with self-calibration, *J. Chromatogr. A*, 2010, **1217**(24), 3896–3899.
47 D. A. Bruzewicz, M. Reches and G. M. Whitesides, Low-Cost Printing of Poly(dimethylsiloxane) Barriers To Define Microchannels in Paper, *Anal. Chem.*, 2008, **80**(9), 3387–3392.
48 F. Ghaderinezhad, *et al.*, High-throughput rapid-prototyping of low-cost paper-based microfluidics, *Sci. Rep.*, 2017, **7**(1), 3553.
49 S. Kasetsirikul, *et al.*, Rapid, Simple and Inexpensive Fabrication of Paper-Based Analytical Devices by Parafilm®, Hot Pressing, *Micromachines*, 2022, **13**(1), 48.
50 Y. S. Kim, Y. Yang and C. S. Henry, Laminated and infused Parafilm® – paper for paper-based analytical devices, *Sens. Actuators, B*, 2018, **255**, 3654–3661.
51 W. Liu, *et al.*, Laminated Paper-Based Analytical Devices (LPAD) with Origami-Enabled Chemiluminescence Immunoassay for Cotinine Detection in Mouse Serum, *Anal. Chem.*, 2013, **85**(21), 10270–10276.
52 C. L. Cassano and Z. H. Fan, Laminated paper-based analytical devices (LPAD): fabrication, characterization, and assays, *Microfluid. Nanofluid.*, 2013, **15**(2), 173–181.
53 J. C. Hofstetter, *et al.*, Quantitative colorimetric paper analytical devices based on radial distance measurements for aqueous metal determination, *Analyst*, 2018, **143**(13), 3085–3090.
54 C. K. Camplisson, *et al.*, Two-ply channels for faster wicking in paper-based microfluidic devices, *Lab Chip*, 2015, **15**(23), 4461–4466.
55 C.-M. Wang, C.-Y. Chen and W.-S. Liao, Enclosed paper-based analytical devices: Concept, variety, and outlook, *Anal. Chim. Acta*, 2021, **1144**, 158–174.
56 M. Anni, Operational lifetime improvement of poly(9,9-dioctylfluorene) active waveguides by thermal lamination, *Appl. Phys. Lett.*, 2012, **101**(1), 013303.
57 H. Kudo, *et al.*, Microfluidic Paper-Based Analytical Devices for Colorimetric Detection of Lactoferrin, *SLAS Technol.*, 2019, **25**(1), 47–57.
58 M. Rutkowska, *et al.*, Low-cost flexible laminated graphene paper solid-contact ion-selective electrodes, *Sens. Actuators, B*, 2021, **337**, 129808.
59 R. J. Crawford and J. L. Throne, 2 – Rotational molding polymers, in *Rotational Molding Technology*, ed. R. J. Crawford and J. L. Throne, William Andrew Publishing, Norwich, NY, 2002, pp. 19–68.
60 X. Lu, *et al.*, Improving interface adhesion of magnetic particle modified EVA hot melt adhesive through introduction of a thermodynamically compatible component, *RSC Adv.*, 2017, **7**(58), 36382–36391.
61 Y.-J. Park, *et al.*, Adhesion and rheological properties of EVA-based hot-melt adhesives, *Int. J. Adhes. Adhes.*, 2006, **26**(8), 571–576.
62 S. S. Soman, D. S. Arathy and E. Sreekumar, Discovery of Anas platyrhynchos avian β-defensin 2 (Apl_AvBD2) with antibacterial and chemotactic functions, *Mol. Immunol.*, 2009, **46**(10), 2029–2038.
63 S. Liu, *et al.*, Directly writing barrier-free patterned biosensors and bioassays on paper for low-cost diagnostics, *Sens. Actuators, B*, 2019, **285**, 529–535.
64 R. Ghosh, *et al.*, Fabrication of laser printed microfluidic paper-based analytical devices (LP-μPADs) for point-of-care applications, *Sci. Rep.*, 2019, **9**(1), 7896.
65 Y. Yang, *et al.*, Paper-Based Microfluidic Devices: Emerging Themes and Applications, *Anal. Chem.*, 2017, **89**(1), 71–91.
66 L. Atkin, Chronic wounds: the challenges of appropriate management, *Br. J. Community Nurs.*, 2019, **24**(Sup9), S26–S32.